

Electrodeposition of BaCO₃ coatings on stainless steel substrates: Oriented growth in the presence of complexing agents[†]

SUMY JOSEPH¹, SARALA UPADHYA² and P VISHNU KAMATH^{1,*}

¹Department of Chemistry, Central College, Bangalore University, Bangalore 560 001

²Department of Mechanical Engineering, University Visvesvaraya College of Engineering, Bangalore 560 001

e-mail: vishnukamath8@hotmail.com

Abstract. Electrodeposition of BaCO₃ from aminocarboxylate stabilized-Ba(HCO₃)₂ baths, results in oriented crystallization when the bath conditions promote the decomposition of the Ba complex. Crystal growth is predominant along the *c*-crystallographic axis. The crystallites orient themselves with their *c*-axis normal to the substrate. The crystallites exhibit three-fold twinning (trilling) consequent to the evolution of the {110} planes as planes of reflection. Pairs of trillings are seen to grow about a four-sided polygon formed by the {010} crystal faces whose centre is a point of inversion.

Keywords. BaCO₃; electrodeposition; oriented crystallization.

1. Introduction

Under biogenic conditions the mineralization of inorganic materials is controlled by a range of biochemical mechanisms. For instance, during biogenesis, an exquisite control over polymorph selection is exercised during the mineralization of CaCO₃.¹ For any chosen polymorph there is further selectivity for size, morphology, aggregation and texture. In biological systems, crystallization onto an organic matrix takes place in presence of acidic macromolecules and dissolved ions that can influence the process. Therefore many investigations to mimic biogenic mineralization have been carried out in the presence of cationic or anionic species,^{2–4} soluble molecular species,^{5–7} polymers^{8–9} or specially designed solid templates.^{10–12} These additives mimic either the structure or function of the naturally existing medium in which biogenesis takes place.

BaCO₃ crystallizes with orthorhombic symmetry. Being the thermodynamically most stable polymorphic modification among the heavy metal carbonates, BaCO₃ synthesis has been studied as a model system for the biogenic crystallization of the aragonite modification of CaCO₃.¹² There is sustained interest in synthesizing BaCO₃ with controlled morphologies. The polymer-assisted template method

was developed as a common method to grow BaCO₃ with controlled morphology.¹³ These templates direct structure, morphology and crystallographic orientation by an interfacial molecular recognition mechanism.

BaCO₃ has important applications in paint, ceramic, and paper industries. Also it is used as starting material for BaTiO₃ synthesis. Decomposition of a biphasic coating of BaCO₃ and TiO₂ resulted in the formation of nano particles of BaTiO₃.¹⁴

On account of its ability to control growth kinetics, electrodeposition has emerged as a versatile synthetic technique for oxides, hydroxides, carbonates and sulphates.^{15,16} Electrodeposition of metal carbonates has generated much interest, since the variable parameters in an electrodeposition directly affect the growth kinetics and properties of the phase that is synthesized. These parameters include deposition current/potential, deposition time, bath composition, pH, level of supersaturation and temperature.

In this paper, we report the electrodeposition of BaCO₃ from different aminocarboxylate-stabilized, Ba²⁺-containing baths. We report the deposition of oriented BaCO₃ crystallites with different morphologies.

2. Experimental

BaCO₃ coatings were deposited by cathodic reduction of a Ba(HCO₃)₂ solution. In order to prevent the

[†]Dedicated to the memory of the late Professor S K Rangarajan

*For correspondence

bulk precipitation of BaCO_3 , Ba^{2+} is complexed with different ligands. Equal volumes of solutions of $\text{Ba}(\text{NO}_3)_2$ (0.05 M), complexing agent (0.05 M) and NaHCO_3 (0.1 M) were mixed in that order. The pH (3.5–7) of the bath was adjusted to a desired value with dilute solutions of NaOH or HNO_3 . All the solutions were prepared using Type I water (specific resistance, 18.2 M Ω cm, Millipore Academic Water purification system). The stability of the bath was verified by allowing the mixture to stand for over 12 h. No bulk precipitation was observed in this period. Stainless steel flags (SS 304, surface area 4.5 cm²) were used as substrates (cathodes) for the deposition. A Pt-mesh (geometric surface area 28 cm²) was used as the anode. A saturated calomel electrode (0.24 V) was used as reference. Current densities ranging from (10 to 30 mA cm⁻²) were employed in the galvanostatic mode (EG & G PARC Versastat model IIA scanning potentiostat driven by model M270 Power ECHM software) for durations of 15–45 min. The cell used was undivided. After deposition, the coating was rinsed with water and dried at 80°C. Prior to electrosynthesis, the working electrode was electrochemically polished as described elsewhere¹⁶.

All coatings were studied by powder X-ray diffraction (PXRD) by mounting the electrode directly on a Bruker Model D8 Advance powder diffractometer, operated in reflection geometry ($\text{CuK}\alpha$, $\lambda = 1.541 \text{ \AA}$). The data were collected at a continuous scan rate of $1^\circ 2\theta$ per minute and then rebinned into 2θ steps of 0.02° . All PXRD profiles were fit by the Rietveld method (FullProf suite), using the published structure of BaCO_3 (ICSD CC 15196, space group: $Pm\bar{c}n$, $a = 5.31 \text{ \AA}$, $b = 8.9 \text{ \AA}$, $c = 6.43 \text{ \AA}$). Anomalous variations in the relative intensities of select Bragg reflections were attributed to the growth of oriented crystallites.¹⁷ These appear as residual intensities in the difference profile obtained at the end of the structure refinement process. The degree of orientation can be quantified by including the Modified March's Function which has two refinable parameters G_1 and G_2 in the refinement process. Of the two, G_2 defines the degree of orientation. $G_2 = 0$ corresponds to a fully oriented coating while $G_2 = 1$ corresponds to a film without any preferred orientation. Scanning electron micrographs were obtained using JEOL Model JSM 6490 LV microscope by mounting a small piece of the BaCO_3 coated electrode on conducting carbon tape and sputter coating with platinum to improve the conductivity.

3. Results and discussion

Metal carbonates are generally obtained by precipitation from a suitable salt solution. The uncontrolled mixing of reagents results in crystallites with ill-defined morphology. Therefore different methods are employed during chemical synthesis to ensure adequate control over the degree of supersaturation, rate of nucleation and growth of the crystallites. A precise maintenance of the pH and temperature is also essential to control crystal growth. A slow release of carbonate ions by urea hydrolysis resulted in the oriented crystallization of BaCO_3 along [001] direction.¹⁸

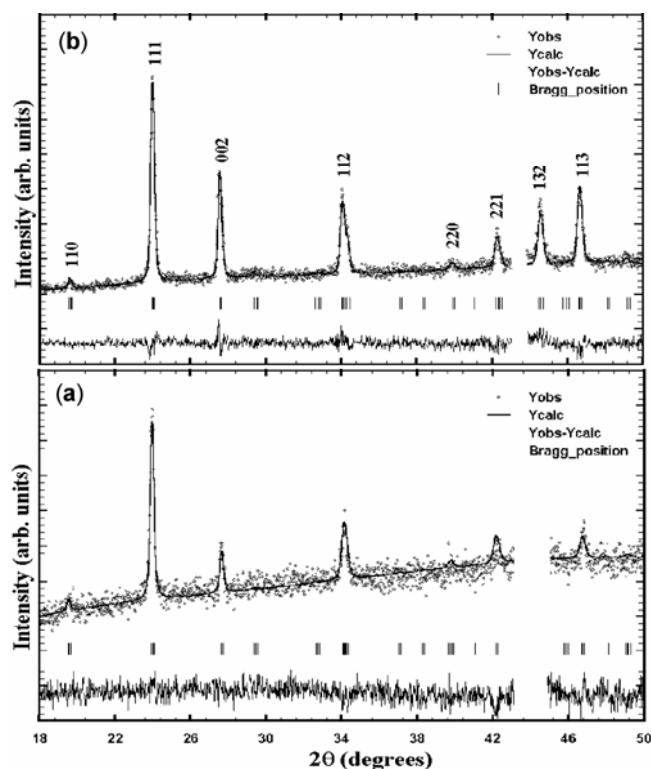
Another method of controlling the kinetics of crystallization is by the use of electrochemistry. For the successful electrosynthesis of any material, it is necessary to have a stable bath comprising the reactant moieties. Since BaCO_3 has a low solubility product (8×10^{-9}), it is necessary to use a complexing agent to prevent chemical precipitation and thereby stabilize the bath. EDTA (ethylenediaminetetraacetic acid) is widely used to complex alkaline earth metals. Electrodeposition yielded oriented coatings of BaCO_3 .¹⁶ In later work on electrodeposition of isostructural SrCO_3 ,¹⁹ the EDTA bath yielded only unoriented coatings. Among other aminocarboxylates, only DTPA (diethylenetriaminepentaacetic acid) yielded an oriented coating of SrCO_3 .

Since the solubility product of SrCO_3 (9.42×10^{-10}) is comparable to that of BaCO_3 , we surmised that the differences between the two systems arise on account of the stability of the various aminocarboxylate complexes with M^{2+} ($\text{M} = \text{Ba}, \text{Sr}$). We therefore investigated the deposition of BaCO_3 from baths stabilized with a number of aminocarboxylates (see table 1). The stability constants of their complexes with Ba^{2+} vary widely over many orders of magnitude. The complex with NTA is least stable, while that with DTPA is the most stable. This is because the structure, coordination geometry and total charge vary between the different molecules in the series.

In figure 1a is given the PXRD pattern of BaCO_3 obtained from an EDTA-stabilized bath ('thin' coating: current 10 mA cm⁻², $t = 15$ min). The Rietveld fit of the observed PXRD profile matches with that calculated for the structure of BaCO_3 (space group $Pm\bar{c}n$). The deposition condition employed is given in table 2. When the deposition was carried out for a longer duration ('thick' coating: $t = 30$ min), there

Table 1. Structure of the complexing agents used and the stability constants of their complexes with Ba²⁺.

Complexing agent	Structure	log <i>K</i> _{MY}
NTA (Nitrilotriacetic acid)	$\begin{array}{c} \text{CH}_2\text{COOH} \\ \diagup \\ \text{N} \\ \diagdown \\ \text{CH}_2\text{COOH} \\ \text{CH}_2\text{COOH} \end{array}$	5.30
EDTA (Ethylenediamine tetraacetic acid)	$\begin{array}{ccc} \text{HOOCCH}_2 & & \text{CH}_2\text{COOH} \\ & \diagdown \quad \diagup & \\ & \text{NCH}_2\text{CH}_2\text{N} & \\ & \diagup \quad \diagdown & \\ \text{HOOCCH}_2 & & \text{CH}_2\text{COOH} \end{array}$	7.76
DTPA (Diethylenetriamine pentaacetic acid)	$\begin{array}{ccccc} \text{HOOCCH}_2 & & \text{CH}_2\text{COOH} & & \text{CH}_2\text{COOH} \\ & \diagdown \quad \diagup & & \diagdown \quad \diagup & \\ & \text{NCH}_2\text{CH}_2\text{N} & \text{CH}_2\text{CH}_2\text{N} & & \\ & \diagup \quad \diagdown & & \diagup \quad \diagdown & \\ \text{HOOCCH}_2 & & & & \text{CH}_2\text{COOH} \end{array}$	8.87

**Figure 1.** PXRD patterns and the corresponding Rietveld fits of BaCO₃ coatings obtained from an EDTA stabilized bath at deposition times (a) 15 min (thin) and (b) 30 min (thick coating). The 2θ region containing the features due to the stainless steel substrate is excluded.

was an anomalous growth in the intensity of the 002 reflection. The experimental profile could be fit by Rietveld refinement (figure 1b) by including the March function parameters (table 2) to account for

preferred orientation. The refined value for G_2 was found to be 0.32, indicative of high degree of orientation. These results are in keeping with our earlier observations of increased preferred orientation on increasing the thickness of the deposit.¹⁶

The thickness of the deposit depends on the amount of charge passed, $Q = \text{current density} \times \text{duration of deposition}$. So the Q was kept fixed at 300 mA min/cm², in further experiments. Figure S1 (supplementary information) shows the PXRD patterns of BaCO₃ coatings obtained from NTA and DTPA-stabilized baths respectively. Ba-NTA complex has a stability constant ($\log K_{MY} = 5.30$) lower, while Ba-DTPA has a stability constant ($\log K_{MY} = 8.87$) higher than the Ba-EDTA complex ($\log K_{MY} = 7.76$). The PXRD patterns show that the degree of orientation of the coating obtained from the DTPA-stabilized bath is lower ($G_2 = 0.85$) than that obtained from the NTA-stabilized bath ($G_2 = 0.0$). The Ba-DTPA complex is more stable than the Ba-EDTA complex, but Ba-NTA complex is weaker by several orders of magnitude. There is a definite inverse relationship between the degree of orientation of the BaCO₃ coating and the stability of its complex with the ligating agent.

BaCO₃ deposition is a result of the following reactions:

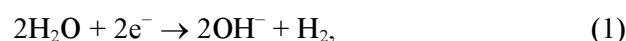
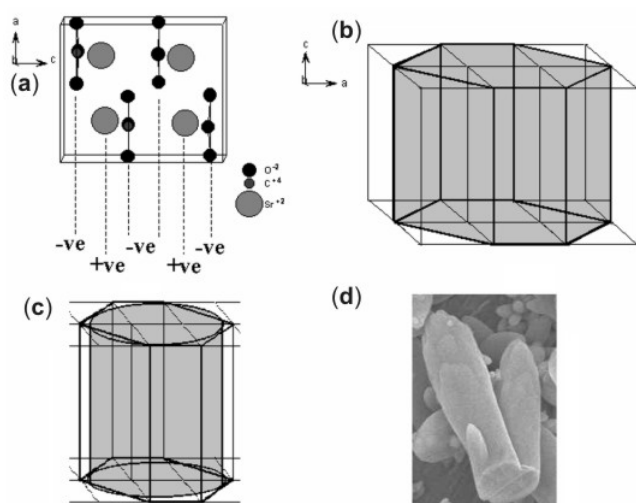


Table 2. A summary of the results of electrodeposition of BaCO₃ coatings from different ligand-stabilized baths.

Ligand (L)	[L]/[Ba ²⁺] ratio	pH	Deposition condition	Orientation <i>G</i> ₁	Parameters <i>G</i> ₂
EDTA	1	5.5	10 mA cm ⁻¹ , 15 min	0.22(1)	0.97(3)
			10 mA cm ⁻¹ , 30 min	0.53(1)	0.32(2)
NTA	1	5.5	10 mA cm ⁻¹ , 30 min	0.38(2)	0.00
			30 mA cm ⁻¹ , 30 min	–	–
DTPA	1	3.5	10 mA cm ⁻¹ , 45 min	0.55(7)	0.00
			10 mA cm ⁻¹ , 30 min	0.39(2)	0.85(3)
		5.5	10 mA cm ⁻¹ , 45 min	0.61(1)	0.01(1)
			10 mA cm ⁻¹ , 45 min	0.39(5)	0.82(0)

**Figure 2.** (a) Projection of the BaCO₃ structure showing the alternation of cationic and anionic layers, (b) a schematic of the pseudohexagonal crystallite of BaCO₃, (c) and (b) with loss of faceting, (d) a typical BaCO₃ crystallite with a columnar morphology (magnification: 1000X).

Of these, reaction (1) called electrogeneration of base is electrochemically controlled. The kinetics of release of OH⁻ ions is controlled by the cell current and the total amount of base generated depends on the charge passed, *Q*. These have been kept constant in deposition experiments with different ligating agents. Reaction (2) is purely chemical and since the [HCO₃⁻] concentration is maintained invariant in all the experiments, the amount of CO₃²⁻ ions generated is also the same. The kinetics of BaCO₃ deposition is then solely dependent on the equilibrium constant of reaction (3). If the [Ba–L] complex is strong, the free Ba²⁺ concentration is low, slowing down the

rate of deposition. A slow reaction invariably leads to a thermodynamically stable state. In the present instance, thermodynamic stability is manifested in an unoriented deposit. Ba–NTA complex is the weakest and the resultant rapid deposition yields a coating with a high degree of orientation.

The free Ba²⁺ concentration in the DTPA-stabilized bath can also be varied by varying the bath pH. The stability constant of the Ba-aminocarboxylate is high at higher pHs, and progressively decreases at acidic pH. Therefore at pH 3.5, the equilibrium of reaction (3) shifts to the right and the consequent rapid deposition yields a coating with a high degree of orientation (*G*₂ = 0) (figure S2a). In figures S2b and S2c (see www.ias.ac.in/chemsci; for supplementary information) are shown coatings obtained from baths of pH 5.5 and 7.0 respectively. As the bath pH increases, the degree of orientation comes down (pH 5.5: *G*₂ = 0.010; pH 7: *G*₂ = 0.82). Under extreme deposition conditions, such as high current density (30 mA cm⁻², 30 min) the coating is highly oriented (figure S3) and could not be refined.

As the crystallization of BaCO₃ has not been studied earlier, the crystallization of the isostructural aragonite modification of CaCO₃ is a good model system. Aragonite crystallizes with a characteristic needle morphology, with the long axis parallel to the *c*-crystallographic axis.²⁰ SrCO₃ also belonging to the orthorhombic crystal system, grows as elongated columns, the long axis of the column being parallel to the *c*-crystallographic axis. The orthorhombic structure of the heavy metal carbonates comprises alternate layers of planar carbonate ions and M²⁺ ions stacked along the *c*-axis (figure 2a). This makes the 001 plane polar, thereby accelerating growth along the [001] direction. Such a growth suppresses the 001 crystal face and the crystallites are faceted by other planes, notably those normal to the 001

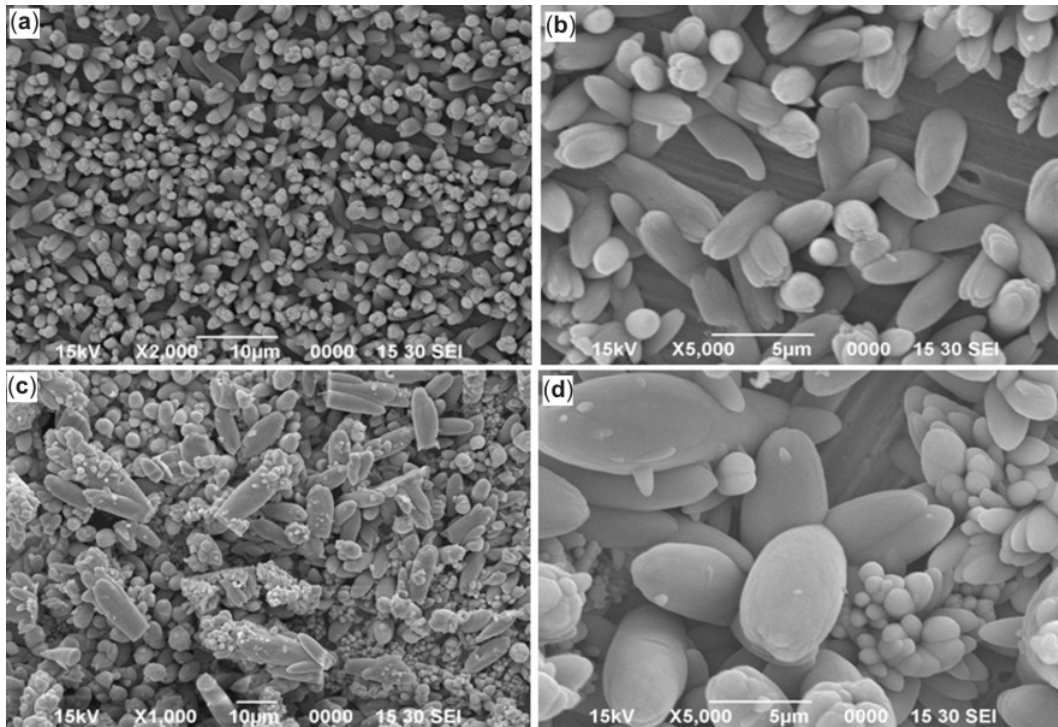


Figure 3. (a, b) SEM images of thin (unoriented) and (c, d) thick (oriented) coatings of BaCO₃ obtained from an EDTA stabilized bath. The corresponding PXRD patterns are given in figure 1.

plane, indexable as $hk0$. The SrCO₃ crystallites have a pseudo-hexagonal symmetry,²¹ and the columnar crystallites are faceted by the $\{110\}$ and $\{010\}$ planes (figure 2b). In keeping with these observations, the BaCO₃ crystallites obtained from the EDTA stabilized bath also have a columnar morphology (figure 3). The columns are truncated at one end and tapered at the other end. The faceting is lost due to re-dissolution in the medium rich in EDTA (schematic in figure 2c). Many of the columnar crystallites are oriented with their long axis normal to the substrate, accounting for the c -axis orientation of the coating (figure 3b). However, a few of the crystallites are oriented with their long axis parallel to the substrate. These exhibit secondary nucleation with each crystallite evolving into a bundle of parallel oriented crystallites.

The coatings obtained from DTPA and NTA stabilized baths also having a c -axis orientation, comprise crystallites which grow normal to the substrate. The outer faces of the crystallites are rounded due to re-dissolution. The crystallites exhibit a three-fold symmetry (figure 4) not observed earlier in similar systems. The observed symmetry of the crystallites is therefore higher than the crystal symmetry. This is

a sign of twinning. Twinning arises when crystal growth takes place simultaneously in two different crystallographic directions from a common nucleus. One of the crystal planes is common to the two crystallites and is called twin plane. The twin plane has the same composition and coordination as in a normal crystal. However, the crystallites on either side of the twin plane are differently oriented.²² Generally, the crystallites on either side of the twin plane are related by some symmetry operation; the twin plane commonly being a plane of reflection. This symmetry element is not a part of the original crystal symmetry.

In figure 4 are shown schematic diagrams which explain the origin of the pseudo three-fold symmetry. Reflection of the pseudo hexagonal crystallites about two adjacent $\{110\}$ planes generates three twins also known as a 'trilling', the line of intersection of the 110 planes of the three twins evolving into a three-fold axis. When two such trillings related by an inversion symmetry grow together, their 010 crystal faces form a four-sided polygon. These morphological features are observed in the SEM images of the coatings obtained from the DTPA and NTA baths.

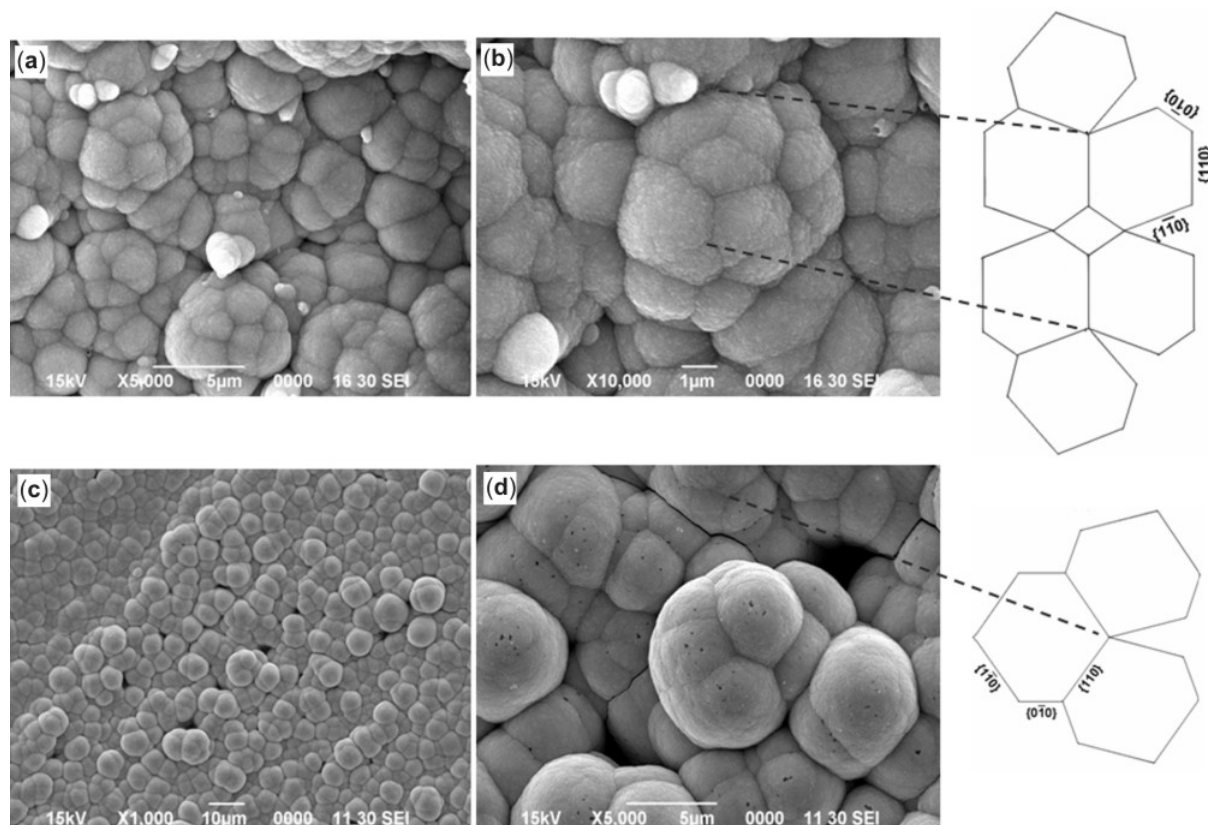


Figure 4. SEM images of BaCO_3 coatings obtained from (a, b) NTA and (c, d) DTPA stabilized bath. The schematic shows a trilling and two trillings observed down the c axis.

4. Conclusions

In conclusion, BaCO_3 coatings are electrochemically deposited from baths stabilized by suitable complexing agents. Strong complexes slow down the rate of deposition and yield unoriented coatings while weak complexes yield oriented coatings. The crystallites grow as three-fold twins. The morphology of the crystallites observed over the micrometer length scale has a basis in the crystal structure of the sub-nanometer length scale. This work has implications for the forces guiding the accretion of atoms over many length scales.

Acknowledgements

The authors thank the University Grants Commission (UGC), for financial support. SJ and PVK acknowledge the Department of Science and Technology (DST), Government of India for the award of Junior Research and Ramanna Fellowships respectively. The authors acknowledge the SEM facilities provided under (TEQIP), funded by World Bank at

University of Visveswaraya College of Engineering (UVCE), Bangalore.

References

1. Addadi L, Joester D, Nudelman F and Weiner S 2006 *Chem. Eur. J.* **12** 981
2. Reddy M M and Nancollas G H 1976 *J. Cryst. Growth.* **35** 33
3. Pytkowicz R M 1965 *J. Geol.* **73** 196
4. Biscoff J L 1968 *J. Geophys. Res.* **73** 3315
5. Mann S, Didymus J M, Sanderson N P and Heywood B R 1990 *J. Chem. Soc. Faraday Trans.* **86** 1873
6. Guo H, Yu J and Cheng B 2006 *J. Solid State Chem.* **179** 2547
7. Shindo H and Kwak M 2005 *Phys. Chem. Chem. Phys.* **7** 691
8. Dousi E, Kallitsis J, Chrissanthopoulos A, Mangood A H and Dalas E 2003 *J. Crystal Growth* **253** 496
9. Ayaé S and Takashi K 2000 *Chem. Commun.* **6** 487
10. Hosoda N and Kato T 2001 *Chem. Mater.* **13** 688
11. Falini G, Fermani S, Gazzano M and Ripamonti A 1997 *Chem. Eur. J.* **3** 1807
12. Mann S, Heywood B R, Rajam S and Birchall J D 1989 *Proc. R. Soc. Lond.* **A423** 457

13. Wang T, Xu A-W and Cölfen H 2006 *Angew. Chem. Int. Ed.* **45** 4451
14. Buscaglia M T, Buscaglia V and Alessio R 2007 *Chem. Mater.* **19** 711
15. Therese G H A and Kamath P V 2000 *Chem. Mater.* **12** 1195
16. Dinamani M, Kamath P V and Seshadri R 2003 *Crystal Growth and Design* **3** 417
17. Joseph S and Kamath P V 2007 *J. Electrochem. Soc.* **154** E102
18. Xu J and Xue D 2006 *J. Phys. Chem. Solids* **67** 1427
19. Joseph S and Kamath P V 2006 *J. Electrochem. Soc.* **153** D99
20. Weiner S and Addadi L 1997 *J. Mater. Chem.* **7** 689
21. Kuther J, Nelles G, Seshadri R, Schaub M, Butt H-J and Tremel W 1998 *Chem. Eur. J.* **4** 1834
22. Giacobazzo C, Monaco H L, Viterbo D, Scordari F, Gilli G, Zanotti G and Catti M 1992 *Fundamentals of crystallography* (Oxford: Oxford University Press)